IMPACT OF ROUGH STOCHASTIC VOLATILITY MODELS ON LONG-TERM LIFE INSURANCE PRICING

Dupret, J-L., Barbarin, J. and D. Hainaut

LIDAM Discussion Paper ISBA/2021/17

UCLouvain

ISBA | LIDAM
Louvain Institute of Data Analysis and Modeling in economics and statistics

Impact of rough stochastic volatility models on long-term life insurance pricing

Jean-Loup Dupret

LIDAM-ISBA, Université Catholique de Louvain, Belgium

Jérôme Barbarin

LIDAM-ISBA, Université Catholique de Louvain, Belgium

Donatien Hainaut

LIDAM-ISBA, Université Catholique de Louvain, Belgium

Abstract

The Rough Fractional Stochastic Volatility (RFSV) model of Gatheral et al. [18] is remarkably consistent with financial time series data as well as with the observed implied volatility surface. Two tractable implementations are derived from the RFSV with the rBergomi model of Bayer et al. [3] and the rough Heston model of El Euch et al. [13]. We now show practically how to calibrate these two rough-type models and how they can price long-term equity-linked life insurance claims. This way, we analyze more closely their long-term properties and compare them with standard stochastic volatility models such as the Heston and Bates model. For the rough Heston, we build a highly consistent calibration and pricing methodology based on a long-term stationary regime for the volatility. This ensures a reasonable behavior of the model in the long run. Concerning the rBergomi, it does not admit a stationary volatility process and hence, this model does not exhibit realistic volatility paths for large maturities. We also show that this rBergomi is not fast enough for calibration purposes, unlike the rough Heston which is highly tractable. Compared to standard stochastic volatility models, the rough Heston hence provides efficiently a more accurate fair value of long-term life insurance contracts embedding path-dependent options while being highly consistent with historical and risk-neutral data.

Keywords: Rough Volatility, Volatility modeling, Equity-linked endowment valuation, Stationary regime, Long-term option pricing, Fractional Brownian motion

1. Introduction

Standard stochastic volatility (SV) models such as the well-known Heston or Bates models have been introduced a while ago to address the shortcomings of the celebrated model of Black & Scholes. However, such models are still limited and cannot reproduce some important empirical facts of the historical volatility time series and of the observed volatility surface.

In their seminal paper, Gatheral et al. [18] propose a model called *"Rough Fractional Stochastic Volatility"* (RFSV) where the process of log-volatility is modeled in terms of a fractional Brownian motion. More precisely, a fractional Ornstein-Uhlenbeck process is

Email address: `jean-loup.dupret@uclouvain.be` (Jean-Loup Dupret)

used with $H < 1/2$, in contrast with the *"Fractional Stochastic Volatility"* model (FSV) previously introduced by Comte and Renault [12], where the Hurst coefficient is assumed to satisfy $H > 1/2$. Gatheral et al. find a highly consistent model with empirical estimates of the volatility time series. More tractable pricing models such as the rBergomi from Bayer et al. [3] or the rough Heston from El Euch et al. [13] were then derived from the RFSV model to improve the efficiency of model calibration and option pricing.

The RFSV model accommodates well for the pricing of long-term equity-linked life insurance contracts. Indeed, as shown in [18], the volatility process σ_t in the RFSV is given by $\sigma_t = \exp(X_t)$, where X_t is the solution of a fractional Ornstein-Uhlenbeck process. Hence, the volatility process in the RFSV is stationary, which ensures a reasonable behavior of the model in the long term. However, we will see that this stationary property will be lost when considering the rBergomi and hence the generated volatility will not exhibit realistic behavior for large times to maturity. For the rough Heston, on the contrary, we will manage to build at large time scales a stationary regime for the volatility in order to ensure reasonableness of the model in the long run and hence price consistently long-term life insurance claims. We will verify practically these long-term properties by valuating an equity-linked endowment embedding a cliquet option (using four different models: Heston, Bates, rBergomi and rough Heston).

The main contribution of this paper is therefore to propose a calibration and a pricing methodology for long-term life insurance contracts using rough-type models. This way, we aim to compute a more consistent and accurate fair value for such long-term claims and highlight the divergent long-term properties between rough volatility models and standard SV models. We will indeed find a significantly different fair value for our equity-linked endowment with models incorporating rough volatility, especially at long time scales with the rough Heston model. This paper also aims to compare these models in terms of fit of the observed European option prices and implied volatility surface, which will confirm the high robustness of rough models. Finally, we contribute with this work to verify the rough behavior of volatility by showing the consistency between risk-neutral and statistical estimation of the Hurst index H, systematically close to 0.1.

2. Life insurance contract

Our aim is thus to price the following equity-linked endowment using rough-type models and compare them with standard SV models, such as the Heston and Bates model. We thus consider an insurance contract which provides a lump sum payment at maturity T in case of survival, or a payment at the time of death t if it occurs before T. We suppose an equity-linked case, where payment amounts depend on the market value of a reference fund $F(t)$ and where an amount $F(0)$ is invested in it at time $t = 0$. We then introduce a **yearly** minimal guarantee κ_g for the policyholder and a maximal **yearly** return κ_m that this policyholder can earn on the fund. The survival benefit is then given by $F^s_T \mathbb{1}_{t \geq T}$ and the death benefit by $F^d_t \mathbb{1}_{t<T}$, where F^e_t for $e = s, d$ is given by a series of guarantees (known as a cliquet option):

$$\begin{aligned} F^e_t = F_0 \prod_{u=1}^{\lfloor t \rfloor} \min\left\{e^{\kappa_m} \,;\, \max\left\{1 + \eta\left(\frac{S_u}{S_{u-1}} - 1\right) \,;\, e^{\kappa_g}\right\}\right\} \\ \times \min\left\{e^{\kappa_m (t-\lfloor t \rfloor)} \,;\, \max\left\{1 + \eta\left(\frac{S_t}{S_{\lfloor t \rfloor}} - 1\right) \,;\, e^{\kappa_g (t-\lfloor t \rfloor)}\right\}\right\} \end{aligned} \tag{2.1}$$

In the equation above, S_t is the price process of each fund unit defined on a filtration $(\mathcal{F}_t)_{t \geq 0}$. The cliquet above implicitly assumes yearly resettlements. Moreover, the rate η

identifies the portion of yearly return recognized to the policyholder with $\eta \in (0, 1]$.

In this life insurance claim, we will model mortality using the following assumptions. We first denote by τ the random residual lifetime of the policyholder aged x at time $t = 0$. We then introduce the non-homogeneous Poisson process $N_t := \mathbb{1}_{\tau<t}$ defined on a filtration $(\mathcal{G}_t)_{t\geq 0}$, which is equal to zero as long as the individual is alive and jumps to one at death. The intensity of N_t is given by the deterministic Makeham force of mortality $\mu_x(t) = c + ab^{x+t}$ and hence her survival probability at time T, being alive at $t = 0$, is equal to :

$$_Tp_x = P(N_T = 0 \,|\, \mathcal{G}_0) = \exp\left(-\int_0^T \mu_x(u)\, du\right)$$

We now introduce the main characteristics of the RFSV model from Gatheral et al. [18] and then derive two tractable models from it, the rBergomi and the rough Heston, that will help us to give a more consistent market value to this insurance contract.

3. Key features of the RFSV model

Gatheral et al. in [18] build the Rough Fractional Stochastic Volatility model (RFSV) with the following SDE under the real-world measure $\mathbb{P}$:

$$dS_t = \mu\, S_t\, dt + \sigma_t\, S_t\, dW_t \tag{3.1}$$

$$d\log(\sigma_t) = \lambda(\eta - \log(\sigma_t))dt + \nu\, dB_t^H \tag{3.2}$$

where μ is a drift term, W_t a standard Brownian motion and B_t^H is a fractional Brownian motion (fBm) with Hurst exponent H. W_t and B_t^H are correlated with a constant correlation ρ such that $\langle W, B^H\rangle_t = \rho t$. Recall that the sample paths of B_t^H are Hölder-continuous of order β for any $\beta > H$. Similarly, sample paths of B_t^H are almost surely nowhere Hölder-continuous of order β for any $\beta < H$. Therefore, the larger the Hurst exponent H, the smoother the sample paths and the lower the H, the rougher they are. More precisely, when $H < 1/2$, the sample paths of the fBm are called rough.

Following Cheridito et al. [11], we have that equation (3.2) models the log-volatility as a fractional Ornstein-Uhlenbeck (fOU) process and we can then use path-wise integration to find the following stationary solution of this fOU process :

$$\log\sigma_t = \eta + \nu\int_{-\infty}^t e^{-\lambda(t-u)} dB_u^H \iff \sigma_t = \exp\left(\eta + \nu\int_{-\infty}^t e^{-\lambda(t-u)} dB_u^H\right) \tag{3.3}$$

One important property of the RFSV is that the volatility process σ_t itself generated by this model is again stationary, which ensures reasonable properties when pricing long-term claims on the underlying.

The cornerstone of [18] is to impose the Hurst exponent H of the fBm B_t^H to be in $\left(0, \frac{1}{2}\right)$ and a very long reversion time scale with $\lambda \ll 1/T$. Such conditions aim to generate rough sample paths and to introduce short-range dependence for the volatility process as we will now see with the two following results. These findings are extremely consistent with empirical statistical properties of the observed volatility time series as verified in Gatheral et al. [18] and Bennedsen et al. [6].

Firstly, these authors show, for $\lambda \ll 1/T$ and $0 < H < 1$, that the log-volatility process $\log\sigma_t$ behaves locally (at time scales smaller than T) as a fBm. Indeed, they prove as $\lambda \to 0$:

$$\mathbb{E}\Big[\sup_{t\in[0,T]} |\log\sigma_t - \log\sigma_0 - \nu B_t^H|\Big] \to 0 \tag{3.4}$$

and that :

$$\mathbb{E}[|\log\sigma_{t+\Delta} - \log\sigma_t|^q] \to \nu^q\, K_q\, \Delta^{qH} \tag{3.5}$$

where $q > 0$ and where K_q is the moment of order q of the absolute value of a $N(0,1)$ random variable. Hence, when λ is small, we have under the RFSV model (3.2) that the log-volatility is close to the fBm B_t^H and is hence still locally Hölder continuous of exponent β for all $\beta < H$. Furthermore, this model approximately reproduces the well-known scaling property of the fBm (Karatzas and Shreve [22]). This scaling property (3.5) is clearly verified empirically for the discrete spot log-volatility process and allows us to estimate the Hurst index H of the observed volatility process. Many studies (as in [6]) consistently find $H \approx 0.1$, which confirms the rough property of the historical volatility, *i. e.* a Hurst exponent $H < 1/2$.

Secondly, neither the autocorrelation function (acf) of the observed empirical volatility nor the acf of the volatility process generated by the RFSV decay as a power law. This contradicts the widespread belief of long-range dependence of the empirical volatility process (as in Andersen et al. [1]). Therefore, Gatheral et al. [18] claim that the historical data are in accordance with the RFSV and the absence of long-range dependence of the volatility process.

Finally, the RFSV model is not only consistent with empirical statistical properties of the volatility time series but also with the observed implied volatility surface. Indeed, standard stochastic volatility models such as the Hull and White and Heston models do not provide a good fit of the volatility surface (especially for short expirations). Particularly, these models generate a term structure of at-the-money (ATM) volatility skew[1] under a risk-neutral measure $\mathbb{P}^*$ that do not match the observed one for small time to maturity τ. Instead, empirical studies show that this observed term structure of ATM skew is well approximated by power-law functions of the form $\psi(\tau) \sim \tau^{H-1/2}$ with $0 < H < 1/2$, which can be generated by stochastic volatility models where the log-volatility is driven by fBm with values of the Hurst exponent in $(0, 1/2)$. The explosion of the volatility skew as $\tau \to 0$ can therefore be modeled using fBm without introducing jumps in our model, as we will confirm in Section 5.

Although empirically and theoretically grounded, the RFSV does not allow to price rapidly option prices and therefore to calibrate effectively a pricing model. Indeed, we need Monte-Carlo simulations which are fairly slow, especially for calibration. Therefore, we now show how to adapt the RFSV to obtain more tractable models that can be used to price long-term claims on the underlying. We first analyze in more details a simple case of the RFSV model when $\lambda = 0$, the rBergomi model, built upon a forward variance curve. Secondly, we study an extension of the classical Heston model incorporating a rough fractional volatility process. This rough Heston model has the nice property of generating a realistic long-term behavior for the volatility process and of having a characteristic function of the log-stock price in quasi-closed form.

[1] Recall that the term structure of ATM volatility skew is defined by $\psi(\tau) := |\frac{\partial}{\partial K}\hat{\sigma}_t^{imp}(K,\tau)|_{K=S_t}$ with $\tau = T - t$.

3.1. rBergomi model

First, let denote $v_u = \sigma_u^2$ the instantaneous variance at time u and the forward variance curve (also called variance swap curve) $\xi_t(u) = \mathbb{E}[v_u|\mathcal{F}_t]$, $u \geq t$. We can easily recover v_t from $\xi_t(u)$ as $v_t = \lim_{u\to t} \xi_t(u)$. Following Bergomi and Guyon [8], forward variance models are models that can be written as a function of this curve $\xi_t(u)$.

In order to build a consistent term structure of volatility skew $\psi(\tau)$ with the empirical one, Bayer et al. [3] impose the following form for the forward variance curve :

$$\xi_t(u) = \xi_0(u)\,\mathcal{E}\left(\nu \int_0^t \frac{d\hat{W}_s}{(u-s)^\gamma}\right) \tag{3.6}$$

where $\mathcal{E}(\Phi) := \exp\left(\Phi - 1/2\,\mathbb{E}[|\Phi|^2]\right)$ with Φ a zero-mean Gaussian process. Indeed, such models generate a term structure of ATM volatility skew of the form $\psi(\tau) = 1/\tau^\gamma$ in accordance with the observed one. Note that $\int_0^t \frac{d\hat{W}_s}{(u-s)^\gamma}$ is known as the *Volterra* fBm with parameter $\gamma = 1/2 - H$ and has, similar to classical fBm, $(H-\varepsilon)$-Hölder sample paths, for any $\varepsilon > 0$.

Following Bayer et al. [3], the Bergomi model (3.6) can be generalized by introducing a fBm B_t^H with $H < 1/2$. This model is called the rBergomi model and it is based on the simplifying assumption $\lambda = 0$ of the RFSV model. These authors show that the variance process v_u in the rBergomi can be rewritten under the physical measure $\mathbb{P}$ as :

$$v_u = \mathbb{E}^{\mathbb{P}}(v_u|\mathcal{F}_t)\exp\left(\eta\,\tilde{W}_t(u) - \frac{1}{2}\mathbb{E}^{\mathbb{P}}\left[|\eta\tilde{W}_t(u)|^2\right]\right) = \mathbb{E}^{\mathbb{P}}(v_u|\mathcal{F}_t)\,\mathcal{E}\left(\eta\tilde{W}_t(u)\right)$$

where $\tilde{W}_t(u) := \sqrt{2H}\int_t^u \frac{d\hat{W}_s}{(u-s)^\gamma}$ and $\eta := 2\,\nu C_H/\sqrt{2H}$ with $C_H = \sqrt{\frac{2H\,\Gamma(3/2-H)}{\Gamma(H+1/2)\,\Gamma(2-2H)}}$.

Under an equivalent measure $\mathbb{P}^*$ where the change of measure λ_t is deterministic and given by $W_t^* = \hat{W}_t - \lambda_t\,t$, we have that W_t^* is martingale under $\mathbb{P}^*$. From that, we finally have for the rBergomi model under $\mathbb{P}^*$:

$$v_u = \mathbb{E}^{\mathbb{P}}[v_u|\mathcal{F}_t]\,\mathcal{E}\left(\eta\,\tilde{W}_t^*(u)\right)\exp\left\{\eta\,\sqrt{2H}\int_t^u \frac{\lambda_s}{(u-s)^\gamma}ds\right\} \tag{3.7}$$

$$= \mathbb{E}^{\mathbb{P}^*}[v_u|\mathcal{F}_t]\,\mathcal{E}\left(\eta\,\tilde{W}_t^*(u)\right) \tag{3.8}$$

$$= \mathbb{E}^{\mathbb{P}^*}[v_u|\mathcal{F}_t]\,\exp\left\{\eta\sqrt{2H}\int_t^u \frac{1}{(u-s)^\gamma}dW_s^* - \frac{\eta^2}{2}(u-t)^{2H}\right\} \tag{3.9}$$

$\mathbb{E}^{\mathbb{P}^*}[v_u|\mathcal{F}_t]$ is the forward variance curve $\xi_t(u)$ observed on the market. It is important to note the presence of the Volterra fBm in equation (3.9) with $\gamma = 1/2 - H > 0$ that induces the rough behavior of the variance process v_u . However, since $\mathbb{E}^{\mathbb{P}^*}[v_u|\mathcal{F}_t] \neq \mathbb{E}^{\mathbb{P}^*}[v_u|v_t]$, this model is non-Markovian. Nevertheless, given the state vector $\xi_t(u)$, which can in principle be computed from observed option prices, the dynamics of the model are well-determined. Finally, the pricing model to be simulated under $\mathbb{P}^*$ is :

$$\begin{aligned} S_T &= S_0\,e^{rT}\,\mathcal{E}\left(\int_0^T \sqrt{v_u}\,dW_u^{*,S}\right) \\ v_t &= \xi_0(t)\,\mathcal{E}\left(\eta\,\tilde{W}_t^*\right) = \mathbb{E}^{\mathbb{P}^*}[v_t|\mathcal{F}_0]\,\mathcal{E}\left(\eta\,\tilde{W}_t^*\right) \end{aligned} \tag{3.10}$$

where $W_t^{*,S} = \rho\,W_t^* + \sqrt{1-\rho^2}\,W_t^{'*}$ and $W_t^{'*}$ a Brownian motion under $\mathbb{P}^*$, independent from W_t^*. We can hence model the leverage effect in the rBergomi model by anticorrelating the Brownian motion that drives the volatility process with the Brownian motion driving the price process with $\rho < 0$.

It is important to note that the assumption $\lambda = 0$ prevents us from having a stationary model for the volatility σ_t. Stationarity being desirable both for mathematical tractability and also to ensure reasonableness of the model at very large times, we will prefer using models with stationary volatility process[2] when pricing long-term financial product, as shown in the next sections.

3.2. Rough Heston

A reminder of the standard Heston model is given in Appendix 10.2. One can show that this Heston model can be written in terms of the forward variance curve $\xi_t(u)$ as in Guyon and Bergomi [8] :

$$d\xi_t(u) = \nu e^{-\lambda(u-t)} \sqrt{v_t}\, d\hat{W}_t^* \tag{3.11}$$

Furthermore, from the classical Mandelbrot-van Ness [24] representation of the fBm, we clearly see that the kernel $(u-s)^{H-1/2}$ plays a central role in the rough dynamic of the fBm with $H < 1/2$. Indeed, as said above, one can show that the Volterra fBm $\int_0^t (u-s)^{H-1/2}\, d\hat{W}_u^*$ has Hölder regularity $H - \varepsilon$ for any $\epsilon > 0$. Therefore, in order to allow for a rough behavior of the volatility in a Heston-type model, El Euch and Rosenbaum [14] naturally introduce the Volterra kernel $(u-s)^{H-1/2}$ in the risk-neutral pricing equation of the Heston model as follows :

$$v_u = v_t + \frac{\lambda}{\Gamma(H+1/2)} \int_t^u \frac{\theta^t(s) - v_s}{(u-s)^{1/2-H}}\, ds + \frac{\nu}{\Gamma(H+1/2)} \int_t^u (u-s)^{H-1/2} \sqrt{v_s}\, d\hat{W}_s^* \tag{3.12}$$

where $\theta^t(.)$ is assumed to be continuous, $\mathcal{F}_t$-measurable and represents a time-dependent mean reversion level. When $H = 1/2$, we can verify that we indeed recover the classical Heston model (10.3). It can also be shown that the trajectories of the volatility itself are almost surely Hölder-continuous of order $H - \varepsilon$, for any $\varepsilon > 0$.

Moreover, El Euch et al. [13] show that under the perfect hedging scheme, $\lambda\theta^t(.)$ can be directly inferred from the forward variance curve observed at time t on the market. By doing so, we can write model (3.12) as:

$$v_u = \xi_t(u) + \frac{1}{\Gamma(H+1/2)} \int_t^u (u-s)^{H-1/2} \nu \sqrt{v_s}\, d\hat{W}_s^* \tag{3.13}$$

Since the forward variance curve $\xi_0(u)$ at time $t = 0$ is observed (or at least can be retrieved) from the market, we only have three parameters left to estimate : H, ν and ρ. Reduction of parameters for the rough Heston is of utmost importance for improving the efficiency of the calibration methodology. Moreover, we note that the limit $u \to t$ of the rough Heston makes no sense. This reflects the fact that this model (as the rBergomi) is not Markovian with respect to the current variance state v_t. However, it is directly visible from equation (3.13) that the rough Heston is Markovian in the forward variance curve $\xi_t(u)$. Finally, the rough Heston can also be expressed in the forward variance form as :

$$d\xi_t(u) = \frac{\nu}{\Gamma(H+1/2)} (u-t)^{H-1/2} \sqrt{v_t}\, d\hat{W}_t^*$$

which is highly similar to (3.11), with the presence of a Volterra kernel in addition.

[2] Note that the Heston and Bates models are examples of model with stationary volatility process (and more precisely, a CIR process).

It is fundamental to note that model (3.13) is not a simplification of model (3.12) obtained by setting $\lambda = 0$ as in the rBergomi model. Instead, it is an equivalent representation of the model (3.12), which comes from the fact that in a perfect hedging scheme, we have :

$$\lambda\theta^0(t) + v_0 \frac{t^{-\alpha}}{\Gamma(1-\alpha)} = D^\alpha\left(\xi_0(t)\right) + \lambda\,\xi_0(t)$$

as shown in El Euch et al. [13] with $\alpha = H + 1/2$. This means that a long-term stationary regime for the volatility process in the rough Heston can be achieved by assuming that $\lim_{t\to\infty} \xi_0(t) = cst$. This way, we avoid an explosion of the initial forward variance term structure $\xi_0(t)$ for large maturities. Long-term stationary regime for the rough Heston will be discussed more thoroughly in the next section.

Furthermore, from Gatheral and Keller-Ressel [19], we have that the forward variance models of Heston and rough Heston are said to be affine. In such cases, they show that the characteristic function of the log-asset price $X_T = \log S_T$ at time t can be written as :

$$\Phi_t(u,T) = \mathbb{E}\left[e^{iuX_T}|\mathcal{F}_t\right] = \exp\left(iu\left(X_t + r(T-t)\right) + \int_t^T \xi_t(s)\, g(T-s, iu)\, ds\right)$$

where $g(t,u)$ is called the Riccati equation. In the classical Heston model, we have with $a = iu$ that :

$$g(t,iu) = \partial_t\, h(t,a) + \lambda\, h(t,a)$$

where :

$$\partial_t\, h(t,a) = -\frac{1}{2}a(a+i) - (\lambda - i\rho\,\nu\, a)h(t,a) + \frac{1}{2}\nu^2\, h(t,a)^2$$

In the rough Heston model with $\lambda = 0$ (and again $a = iu$), we have that :

$$g(t,iu) = D^\alpha h(t,a) = -\frac{1}{2}a(a+i) + i\rho\,\nu\, a\, h(t,a) + \frac{1}{2}\nu^2 h(t,a)^2 \tag{3.14}$$

with D^α the Rieman-Liouville fractional derivative of order $\alpha = H + 1/2$. This equation is exactly the same as in the classical Heston model (with zero-mean reversion) but with the time derivative replaced by a fractional derivative that makes the model rough.

To solve the rough Heston Riccati equation (3.14) and find the solution $h(t,a)$, we use the method described in Gatheral & Radoičić [20] built upon the combination of a short-time expansion of the solution and an asymptotic expansion of the solution when $\tau = T - t \to \infty$. This method is particularly fast, simple and accurate to compute approximate solutions of fractional ordinary differential equation. We can therefore obtain a characteristic function of the log-asset price under the rough Heston in quasi-closed form and then price efficiently European options using the Carr-Madan formula (cfr Appendix (10.1)) combined with a Fast Fourier Transform algorithm.

4. Calibration

In this section, we will build a calibration methodology and compare four models (Heston, Bates, rBergomi and rough Heston) in terms of fit of the observed European option prices and implied volatility surface for the CAC 40 index. We will mainly focus on the long-term behavior of such models and then use these calibrated models to price our long-term life insurance contract embedding the cliquet option (2.1).

We first provide a statistical estimation of the RFSV parameters based on historical data for the CAC 40 index from January 2004 to July 2020 (obtained from the Oxford-Man Institute). Using the scaling property (3.5) as in Gatheral et al. (2014) to estimate the smoothness of the volatility process for the CAC 40, we find an estimated value $\hat{H} = 0.129$. The historical estimate of ν is also derived from (3.5) and is equal to $\hat{\nu} = 0.30977$.

The aim of the calibration method is to find, for each model, the model parameters that match derivative model prices as best as possible with the observed market prices of vanilla derivatives in the market. It then boils down to an optimization problem where we have to find the minimum distance between model prices/model-based implied volatility and market prices/market implied volatility. In this paper, we choose to minimize the distance between model-based implied volatility $\widehat{\sigma}_j^{imp}$ and market implied volatility σ_j^{imp} since it leads to more stable results. Finally, we introduce the weighted Root Mean Square Error as the loss function, which is defined as :

$$\text{RMSE} = \sqrt{\sum_{j=1}^{N} w_j \left(\sigma_j^{imp} - \widehat{\sigma}_j^{imp}\right)^2} \tag{4.1}$$

where $w_j = \frac{1}{\text{Ask}_j - \text{Bid}_j}$, *i. e.* the weight is the inverse of the bid-ask spread, expressed in terms of implied volatility. This way, we give more importance to observations with small bid-ask spread. Indeed, if an option is liquid, then its bid-ask spread is supposed to be small and its price/implied volatility is more accurate. Mathematically, it boils down to find the optimal set $\Theta^* \in \mathbb{R}^p$ of the p model parameters such that :

$$\Theta^* = \arg\min_{\Theta} \mathcal{L}\left(\sigma^{imp}, \widehat{\sigma}^{imp}(\Theta)\right)$$

where $\mathcal{L}$ is the RMSE loss function. Finally, we highlight the fact that the result of this optimization procedure can be highly dependent on the initial parameters. We then use a grid search method for picking the initial parameters that minimize the loss function.

4.1. Market data

We first choose as starting date $t = 0$, the 6^{th} of July 2020. The maturity of vanilla options as well as the risk-free term structure will be defined with respect to this date.

Firstly, the risk-free rates used for pricing purposes are derived from the observed swap term structure. The technique for constructing this swap term structure divides the curve into two term buckets. The short end of the swap term structure is built using interbank deposit rates. We will here consider EURIBOR rates from one day to 12 months. The long end of the risk-free interest rate curve (maturity above 1 year) will be based on the European swap term structure available from the EIOPA for the month of July[3]. Table12.1 in Appendix provides a summary of the risk-free rates used between 0 and 20 years. The dividend yield is chosen to be 1% but this assumption does not have a significant impact on the results and conclusions of this paper.

Secondly, we have that the price S_0 at time 0 of the CAC40 index is equal to 5028.56 €. As mentioned above, we also need market prices of European options on the CAC40 in order to calibrate later our model. From Bloomberg, we gather a database that includes 366 options with the option bid price and the option ask price for different strikes and maturities. The true market price is here considered as the mid value between the bid

[3]Further information on risk-free rates computation can be found at : `https://www.eiopa.europa.eu/tools-and-data/risk-free-interest-rate-term-structures_en`

price and the ask price, which is a common assumption. Using the one-to-one relationship between market prices and implied volatility from the Black and Scholes formula, we can build a database with the bid, ask and mid implied volatility for each strike and maturity. We then apply the following common filters as in Moyaert and Petitjean [26] and select the following options :

- **Out-of-the-money options** : Since out-of-the-money options are more actively traded than in-the-money options (as a protection), the quotes on out-of-the-money options are usually more reliable.
- **The bid-ask spread** (on the option prices) is less than 5%. Otherwise, we consider that there is no sufficient liquidity to take the option into account.
- **Maturity** is less than one year. Indeed, options with an expiration date longer than 1 year are rejected for the calibration since they are less sensitive to volatility as explained in [26]. Note that we also reject options with maturity equal to 0.9 years due to data quality issue for this particular maturity.

We have a final database of 140 OTM options for which we can observe the strike, the maturity, the bid, ask and mid implied volatility.

We now turn to the specific calibration method for each of the model. Indeed, even if the general method is the same, the way we price our European options will vary depending on the model.

4.2. Heston and Bates models

We have at disposal for these two models a closed-form for their characteristic function. Then, following Carr and Madan [10], we can compute prices of European options for a whole range of strikes in one run very fast using Fourier inversion as shown in Appendix 10.1. We then just have to iterate on the different maturities to find the optimal parameters of these models.

- **Heston :**

We find a minimal RMSE of 0.11911 with the initial set of parameters (0.1, 1, 0.15, 1.1, -0.6) which leads to the following final parameter values Θ^*:

σ_0^*	λ^*	η^*	ν^*	ρ^*
0.29376	2.91634	0.09666	1.4704	-0.70093

We see that we have a high speed of mean reversion λ^* and a high level of the vol-of-var parameter ν^* which implies large swings in the variance process. We also obtain a large negative correlation between the stock process and the variance process, which is consistent with the leverage effect. Finally, the mean reversion level η^* towards which the variance will converge is 9.76% (which represents a volatility of 31,23%). It is no wonder to obtain this high level of volatility as well as vol-of-var parameter given the state of the economy due to the COVID-19 outbreak in July. Finally, the Heston model with the parameters obtained above leads to Fig. 4.1 when compared to market prices of European options on the CAC 40 index.

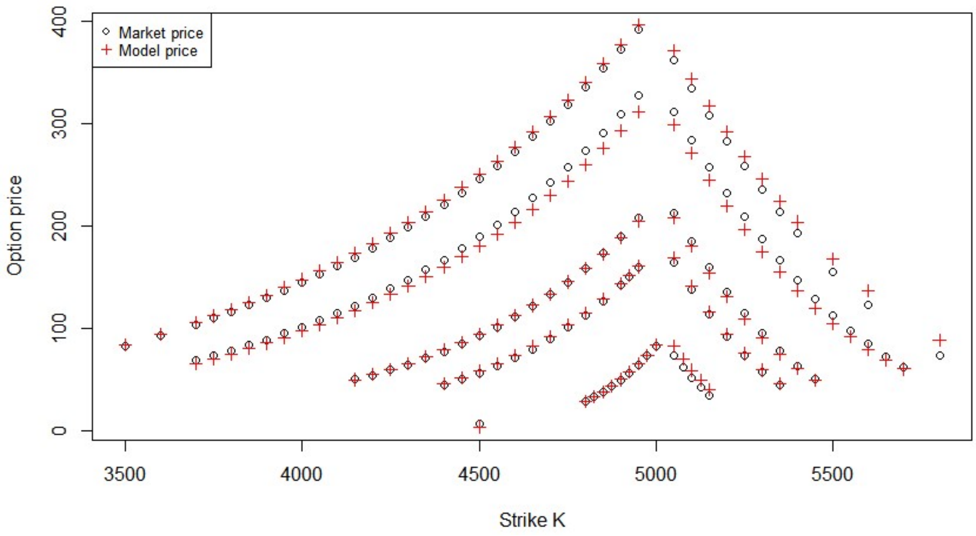

Figure 4.1: Comparison of Heston option prices vs. market option prices (CAC 40)

- **Bates :**

A reminder of the Bates model is given in Appendix 10.3. We then find a minimal RMSE of 0.0852 for the Bates model with the initial set of parameters (0.25, 0.6, 0.1, 0.8, -0.9, 0, 0.1, 0.1). This leads to the following final parameter values Θ^*:

σ_0^*	λ^*	η^*	ν^*	ρ^*	μ_j^*	σ_j^*	λ_j^*
0.2598	0.2498	0.1794	1.140	-0.6644	-0.1045	0.1128	0.8213

Firstly, the RMSE is substantially lower than the one obtained with the Heston model, which means that the Bates model provides a better fit of the observed European option prices. The mean-reversion speed λ^* and the volatility of variance parameters ν^* are also lower, which implies that the swings in the variance process are less pronounced than in the Heston model. Moreover, we now observe jumps in the price process that are on average negative since $\mathbb{E}[Y-1] = e^{\mu_j+\sigma_j^2/2} - 1 < 0$. The annual frequency of these jumps is equal to 82.13%. Finally, we observe that the long-run variance η^* is higher than in the Heston model. This Bates models leads to Fig. 4.2 when compared to the observed market prices. The fit is clearly better than in the Heston model as said above, even if for larger maturities it is not perfect yet.

4.3. Rough Heston calibration

As explained above, we have a quasi-closed form for the characteristic function of the log-price X_t in the rough Heston model. We can then apply exactly the same calibration technique as for the Heston and Bates models described in the previous section. However, recall that the rough Heston is not Markovian in the current variance state v_t but Markovian in the (forward) variance swap curve $\xi_t(u)$. Hence, the rough Heston's characteristic function depends on this variance swap curve. In practice however, the variance swap curve $\xi_0(u)$ at time $t = 0$ is not easily retrieved from the financial markets. Indeed, it is hard to obtain high-quality variance swap data since variance swaps are OTC contracts as explained in [3]. We thus choose to proxy the value of a variance swap of maturity T by the value of a log-contract (also of maturity T) as described for example in Chapter 11 of Gatheral [17]. In a first step, the variance swap curve at time $t = 0$ is therefore calibrated on our database of observed option prices for the CAC 40. We hence obtain the following

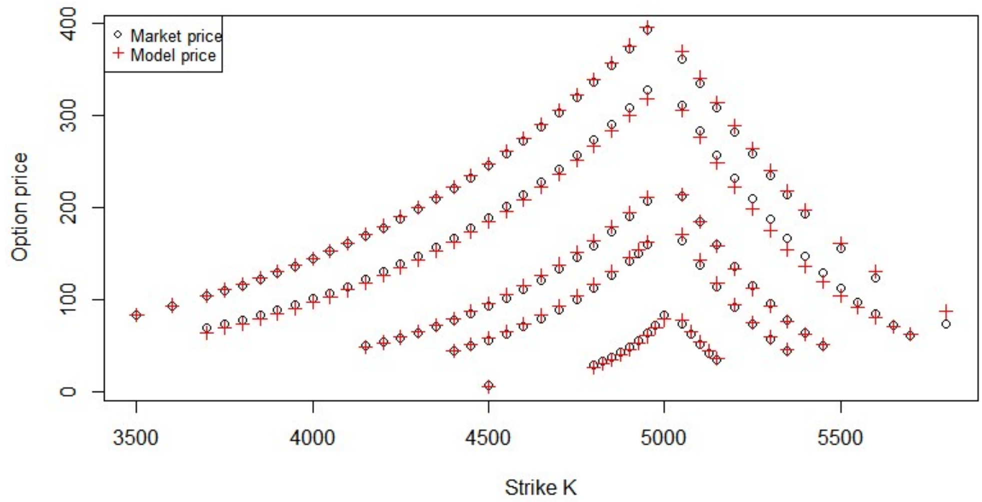

Figure 4.2: Comparison of Bates option prices vs. market option prices (CAC 40)

market variance swap curve $\xi_0(t)$ in Fig. 4.3 between 0 and 1.2 years (when interpolated between observed maturities)[4] .

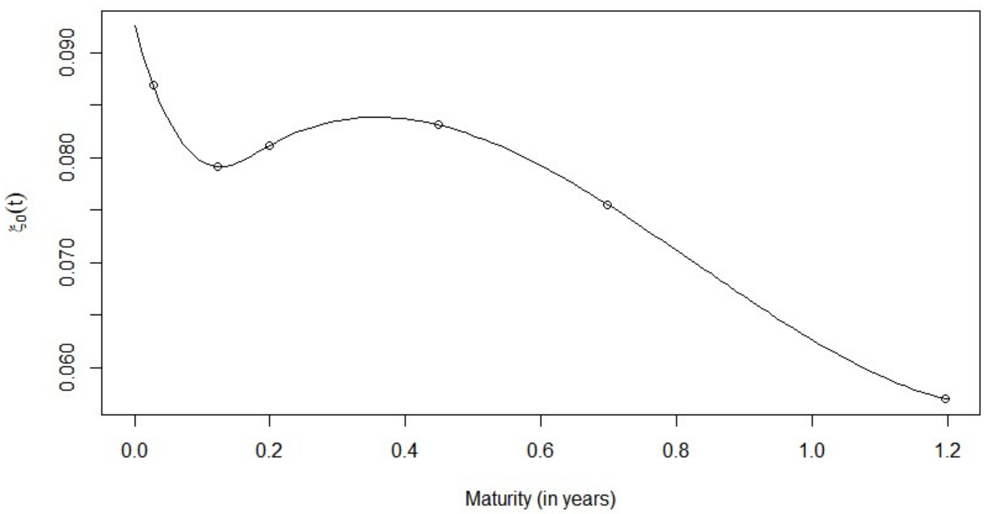

Figure 4.3: Initial forward variance curve $\xi_0(t)$ between 0 and 1.2 years

However, we only have European options with observed maturities until 1.2 years. In order to price long-term claims on the underlying, we need a term-structure parameterisation of our variance swap curve. It is desirable that, in the long run, the values of the initial variance swap curve approach a constant level in order to avoid an explosion of the curve. Therefore, it is reasonable to choose a parameterisation with asymptotic line such that :

$$\lim_{t\to\infty} \xi_0(t) = cst$$

This assumption allows the variance process of the rough Heston to be in a stationary regime when the maturity is large. A classical choice for such parametrisation is the Gompertz function:

$$\xi_0(t) = z_1 e^{-z_2\, e^{-z_3\, t}} \tag{4.2}$$

[4]This time, options with maturity above 1 year were used to derive $\xi_0(t)$ since it ensures a more appropriate and reasonable long-term behavior of the initial forward variance curve.

where z_1 is the asymptote, z_2 sets the displacement along the x-axis (here, the time to maturity) and z_3 sets the growth rate. Fitting the Gompertz function to the observed forward variance curve, we find :

z_1	z_2	z_3
0.03954	-0.7992	0.5672

Therefore, the asymptotic level of the volatility is given by $\sqrt{0.03954} = 19.88\%$. Finally, combining the curve obtained in Fig. 4.3 with the Gompertz fit for $\tau > 1.2$, we obtain the following initial forward variance curve $\xi_0(t)$ in Fig. 4.4. We can observe that we enter a stationary regime as of the 6^{th} year.

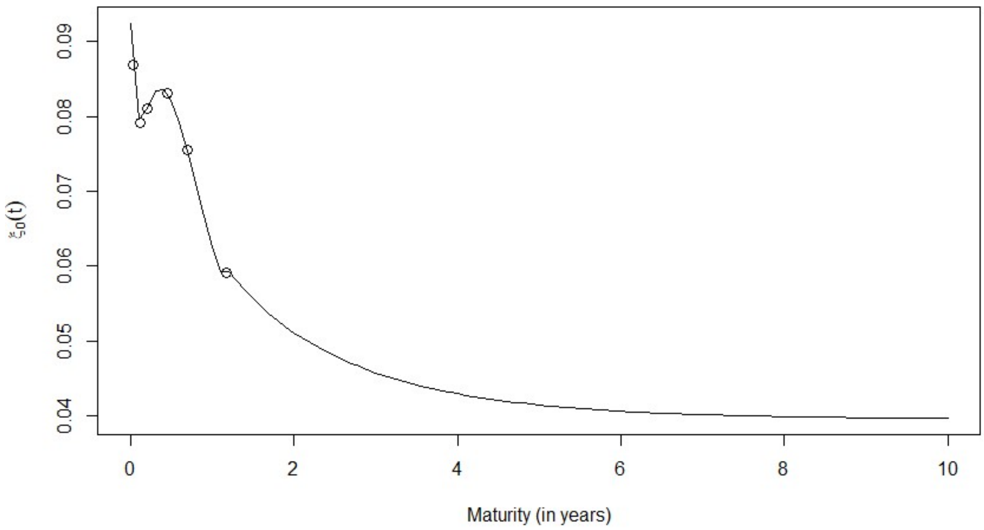

Figure 4.4: Initial forward variance curve $\xi_0(t)$ until $t = 10$ years

However, we are aware that calibrating such Gompertz function based on only 6 different maturity points can seem dubious. Indeed, estimating an asymptotic value for the forward variance from the information carried out by short-maturity option data is not an easy task. The first alternative solution is to use a constant forward variance curve denoted $\xi_0^{cst}(t)$. We decide to fix $\xi_0^{cst}(t) = \xi_0(0) = 0.0925\,,\, \forall t$. Note that this constant level is very close to the long-term mean η^* obtained in the Heston calibration ($= 0.0967$). This will allow us to compare more thoroughly rough-type models with the latter. Results for calibration and pricing with the second forward variance curve $\xi_0^{cst}(t)$ are given in Appendix 11.
Another alternative would have been to keep a Gompertz function for the forward variance curve and find the parameters z_1, z_2 and z_3 such as to minimize the RMSE (4.1) of the model. However, note that this time, the three parameters z_1, z_2, z_3 directly aim to minimize the RMSE and not to fit the market forward variance curve. Hence, the number of effective parameters of the rough Heston (and of the rBergomi) is not 3 anymore but 6 (H, ν, ρ, z_1, z_2, z_3) which leads to instability in the calibration (especially for the rBergomi as explained below). Therefore, we decide not to consider this optimal forward variance curve.

Using again the Carr-Madan formula (10.1) augmented with a FFT algorithm and the numerical approximation of Gatheral & Radoičić [20] for fractional derivatives, we find a RMSE of 0.09235 for the rough Heston with the initial set of parameters (0.05, 0.2, -0.8) and the market forward variance curve $\xi_0(t)$. This leads to the following final values Θ^*:

H^*	ν^*	ρ^*
0.1207	0.4132	-0.8016

Based on the RMSE, we then have a slightly less good fit than with the Bates model. However, recall that the rough Heston has only three parameters to estimate compared with the eight parameters of the Bates model. We will also analyze in the next section which of the models best fits the behavior of the implied volatility surface. Moreover, it is important to note that the Hurst index H^* obtained via the risk-neutral calibration method is consistent with the Hurst index obtained via statistical estimation (under the real-world measure) equal to 0.1292. Yet, we have a higher ν^* than the one estimated based on the historical time series (= 0.3098) due to the market price of risk included in the risk-neutral valuation. Finally, we observe a stronger leverage effect with this model than the previous ones. Fig. 4.5 depicts the fit of the rough Heston options prices compared to the observed market prices of European options.

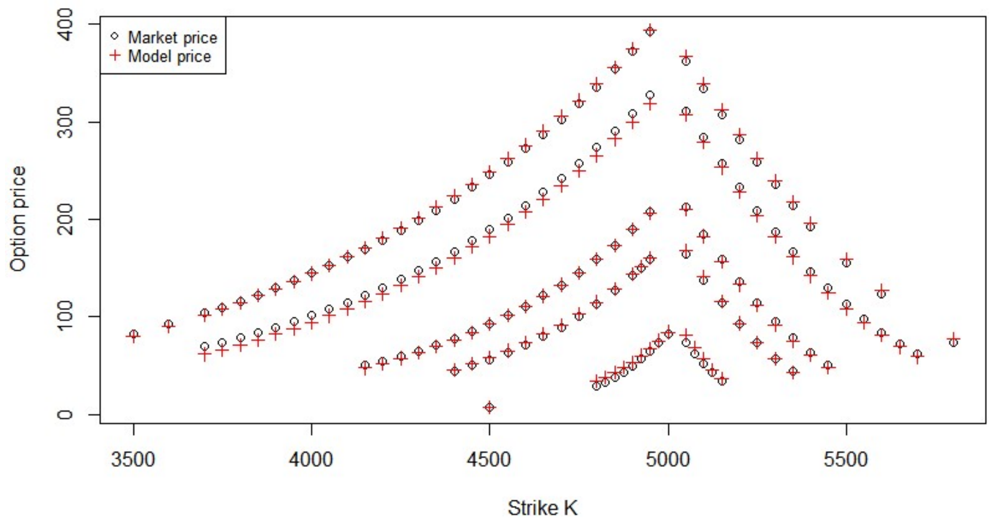

Figure 4.5: Comparison of rough Heston option prices vs. market option prices (CAC 40)

4.4. rBergomi Calibration

The calibration of this model departs significantly from the three models described above. Indeed, no characteristic function is available in (quasi-)closed form. We will then rely on the Hybrid scheme from McCrickerd et al. [25] to calibrate the parameters ρ, η and H of the rBergomi model under $\mathbb{P}^*$. Note that the inital forward variance curve is exactly the same as the one derived in the calibration of the rough Heston model.

This Hybrid scheme uses a Monte-Carlo type approach in order to calibrate the rBergomi model. As for the previous models, we will try to fit as best as possible the observed European option prices. For a parameter set $\Theta = (\rho, \eta, H)$, we simulate m realizations of the variance process and of the price process given in equation (3.10) (more details on the simulation methodology is given in Section 6). We can then compute the price of European calls (and puts in the same way) using :

$$C_0(T,K) = \mathbb{E}^{\mathbb{P}^*}[(S_T - K)^+] = \frac{1}{m}\sum_{i=1}^{m}(S_{T,i} - K)^+$$

We then apply the general calibration method above and the one-to-one correspondence between European option prices and implied volatility to find the model parameters that minimize the distance between model-based implied volatility and market implied volatility. Since the Volterra kernel is a special case of Brownian Semistationary (BSS) processes, we use the papers of Bennedsen et al. [7] and of McCrickerd et al. [25] to improve the efficiency of simulations. They build the following hybrid scheme for the simulation of $\tilde{W}_t(u)$:

$$\begin{aligned}\int_t^u \frac{dW_s}{(u-s)^\gamma} &= \sum_{k=1}^{n} \int_{t_{k-1}}^{t_k} \frac{dW_s}{(u-s)^\gamma} \\ &\approx \sum_{k=1}^{\kappa} \int_{t_{k-1}}^{t_k} \frac{dW_s}{(u-s)^\gamma} + \sum_{k=\kappa+1}^{n} \frac{1}{(u-s_k)^\gamma} \int_{t_{k-1}}^{t_k} dW_s \\ &= \sum_{k=1}^{\kappa} \int_{t_{k-1}}^{t_k} \frac{dW_s}{(u-s)^\gamma} + \sum_{k=\kappa+1}^{n} \frac{1}{(u-s_k)^\gamma} Z_k \sqrt{\frac{u-t}{n}} \end{aligned} \tag{4.3}$$

where $s_k = u - \frac{k}{n}(u-s)$, the Z_k are i.i.d. $N(0,1)$ random variables and the s_k are such that $\int_{t_{k-1}}^{t_k} \frac{ds}{(u-s)^\gamma} = \frac{1}{(u-s_k)^\gamma}$. In practice, $\kappa = 1$ is the best choice. Note that we recover the classical Euler scheme with $\kappa = 0$, which does not perform well in terms of running time.

We find a RMSE of 0.1479 with the initial set of parameters equal to (0.1, 1, 0.85). This leads to the following final values Θ^*:

H^*	η^*	ρ^*
0.1357077	1.4164349	-0.996756

First, the RMSE is higher compared to the three previous model and hence the fit is poorer with the rBergomi. We see that the calibrated Hurst exponent H^* is again very close to the historical estimate. Based on a $\eta^* = 1.416$, we find the corresponding ν^* equal to $\eta^* \sqrt{2H^*}/(2\,C_H) = 0.869$. Therefore, the volatility of variance ν^* clearly needs to be much higher than the historical $\hat{\nu}$ to better fit the European option data (again due to the volatility of variance risk premium). The anti-correlation between the stock process and the variance process is stronger than the ρ^* derived from the rough Heston. Moreover, it is important to add that these results are quite unstable from simulation to simulation. The hybrid scheme is indeed not yet fast enough to provide a reliable calibration method, at least in our implementation. We used $m = 1{,}000{,}000$ and $\Delta t = t_k - t_{k-1} = T/n$ with $n = 400$ and the optimization was done in more than 5 hours with these parameters. We need to increase m and decrease Δt to obtain more precise and stable results but it then requires far more computing time and memory, which is not suitable and tractable in practice. We then obtain Fig. 4.6 where we can see that the OTM puts are substantially off-market with this model.

Finally, recall that our choice of parametrisation for the (market) forward variance curve ensures that in the long term we have on average a constant variance process (equal to 0.0395) in the rBergomi and rough Heston models. Nevertheless, if we now compare the conditional variance of the variance process $\mathbb{V}_{\mathbb{P}^*}[v_u|\mathcal{F}_t]$, we obtain divergent properties between these two models as shown and explained with Fig. 12.1 in Appendix 12.2 and with the corresponding equations 12.1 and 12.2. Clearly, $\mathbb{V}_{\mathbb{P}^*}[v_u|\mathcal{F}_t]$ tends to explode in the rBergomi model which does not allow for a reasonable behavior of the variance process in the long term. On the contrary, the conditional variance $\mathbb{V}_{\mathbb{P}^*}[v_u|\mathcal{F}_t]$ in the rough Heston exhibits an almost constant behavior for large times to maturity and is hence more appropriate for long-term pricing.

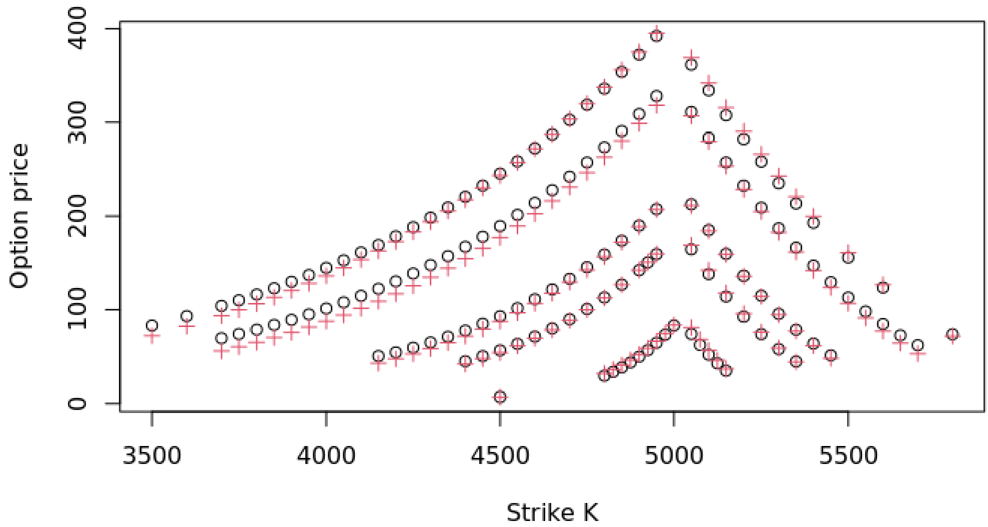

Figure 4.6: Comparison of rBergomi option prices vs. market option prices (CAC 40)

5. Volatility surface fit

We now compare the Heston, Bates, rough Heston and rBergomi models in terms of implied volatility surface fit. More precisely, we will look at the fit of the term structure of ATM volatility skews $\psi(\tau)$ and confirm that rough models provide a better fit.

From our market option prices database, we can build the term structure of ATM volatility skews $\psi(\tau)$. First, recall that $\psi(\tau) := \left|\frac{\partial}{\partial K}\hat{\sigma}_t^{imp}(\tau, K)\right|_{K=S_t}$. We can approximate it for $t = 0$ by :

$$\widehat{\psi}(\tau) = \left|\frac{\hat{\sigma}_0^{imp}(\tau, K+\delta) - \hat{\sigma}_0^{imp}(\tau, K-\delta)}{2\delta}\right|_{K=S_0}$$

for small enough δ and for each available time to maturity $\tau = T - 0$. We then obtain in Fig. 5.1 the term structure of ATM volatility skews for our data. The red dots are the

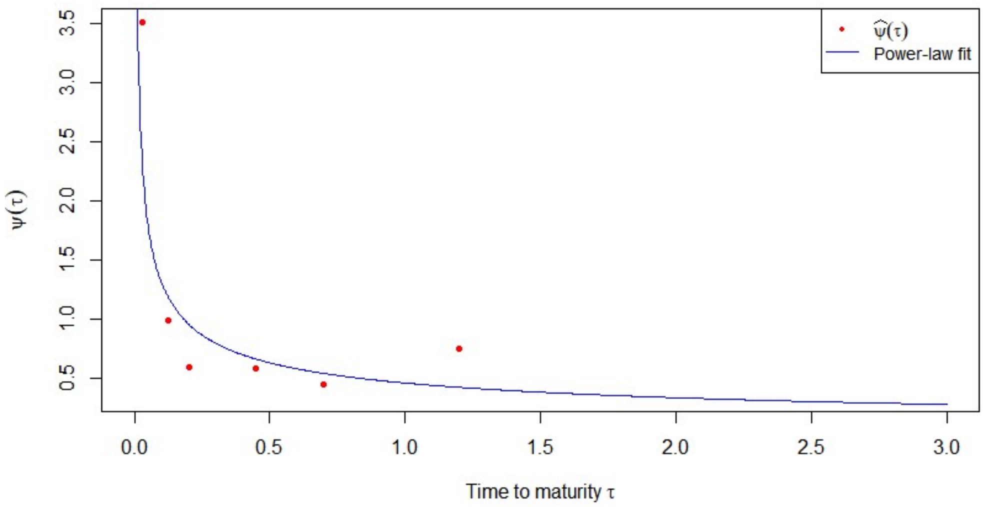

Figure 5.1: Observed ATM volatility skew term structure $\widehat{\psi}(\tau)$ for the CAC 40 in red with the power-law fit superimposed in blue

estimated ATM skews for each of the available maturities. We clearly see that we obtain an ATM volatility skew which is consistent to the power-law function. Indeed, the blue line is the power-law fit to the data, obtained by the following linear regression :

$$\log \psi(\tau) = -\alpha \log \tau$$

We find $\hat{\alpha} = 0.4546$. From Section 3,we know that $\psi(\tau) \sim \tau^{H-1/2}$ holds for the RFSV model. Hence, we have that $\hat{H}_{ATM} = 1/2 - \hat{\alpha} = 0.0452$, which is lower than the Hurst exponent estimated with historical data (but again rough !). However, we do not have a lot of different maturities in our option data set, which prevents us from having a consistent estimator $\hat{H}_{ATM}$ using this power-law fit. Therefore, we will focus our analysis on the shape of the ATM skew term structure and on whether our different models are able to approximate this blue line rather than on the exact fit.

5.1. Comparison of the fit

We now compare the empirical term structure of ATM volatility skews with the term structures derived for each of our models. We first analyze the fit of the Heston and Bates model thanks to Fig. 12.2 in Appendix. The blue line is again the power-law fit of the observed market implied volatility (with $\hat{\alpha} = 0.4546$). The green dots are the $\widehat{\psi}(\tau)$ derived from the Heston model for the available maturities. For the Heston model, we clearly observe that it does not allow to capture the high ATM skews for short maturities and hence the power-law shape of $\psi(\tau)$. This was indeed one of the issue of this model that we rose in Section 3. We can however note that for $T > 0.20$, the Heston model fit approximates quite well the empirical blue line. Concerning the Bates model, the presence of jumps only provides a slightly better fit of the ATM skew $\psi(\tau)$ compared to the Heston model. Indeed, the Bates model is still not able to capture the explosion of the skew for very short expiration. This is due to the fact that the parameter λ controlling the frequency of jumps is only of 0.82 and that the average size of the jumps is also rather low. A higher value of λ or of $|\mu_j|$ would allow to better capture this explosion phenomenon for $\tau \to 0$.

We now analyze the fit of the rough Heston and the rBergomi since we said that rough-type models should be able to better capture the high curvature of $\psi(\tau)$ for small time to maturity thanks to the rough behavior of their volatility process. We obtain Fig. 12.3 in Appendix. We clearly see that the green dots of both figures (*i. e.* the rough Heston and rBergomi fit for available maturities) exhibit the same shape as the blue line and can therefore be fitted by a power-law function $\tau^{H-1/2}$. If we had at disposal even shorter maturities, the rough Heston and rBergomi models would likely better capture the explosion of $\widehat{\psi}(\tau)$ for $\tau \to 0$. We can finally conclude that rough-type models are more consistent with the empirical implied volatility surface than standard SV models.

6. Simulation and discretization methodology

In order to price the above equity-linked life insurance contract, we first need to explain how we can discretize and simulate sample paths of the price process and the variance process under our different models.

- Heston :

Once the Heston model has been calibrated and the optimal parameters $\sigma_0, \lambda, \eta, \nu$ and ρ have been found, we can use a Monte Carlo approach to simulate the sample paths of the Heston model. We first simulate the stock price process and the volatility process by generating correlated $N(0,1)$ random numbers ε_S and ε_v (with correlation ρ). The relationship between ε_S and ε_v can be written as :

$$\varepsilon_{v,t_i} = \rho\ \varepsilon_{S,t_i} + \sqrt{1-\rho^2}\ \varepsilon'_{t_i}$$

where ε_{S,t_i} and ε'_{t_i} are independent $N(0,1)$ random variables. Using an Euler discretization scheme for the price process and the variance process, we have :

$$S_{t_{i+1}} = S_{t_i}\left(1 + r\Delta t + \sqrt{v_{t_i}}\sqrt{\Delta t}\,\varepsilon_{S,t_i}\right) \tag{6.1}$$

$$v_{t_{i+1}} = v_{t_i} + \lambda(\eta - v_{t_i})\Delta t + \nu\sqrt{v_{t_i}}\sqrt{\Delta t}\,\varepsilon_{v,t_i} \tag{6.2}$$

for $i = 0, ..., n-1$, with $t_0 = 0$ and $t_n = T$, where n is the number of time steps and $\Delta t = T/n$, for a given maturity T. We then simulate m sample paths of this stock price process and of this volatility process. Now that we have the full path of $(S_{t_i})_{i=0,...,n}$ for each m, we can price path-dependent options, such as the cliquet option (2.1). In practice, the variance can become negative under a simulation because of the discretization. We then use the full truncation scheme of Lord et. al [23] to tackle this problem since it overcomes other Euler fixes (absorption, relfection, etc.) and quasi-second order schemes (Milstein scheme, Ninomiya and Victoir scheme [27], etc.) in terms of positive bias. The full truncation scheme therefore better reproduces the true properties of the CIR process. This simulation methodology gives us the following Fig. 6.1, depicting one sample path of the variance process under the Heston model over 10 years. We can clearly see the effect of the high volatility of variance (vol-of-var) parameter ν with large swings in the variance process.

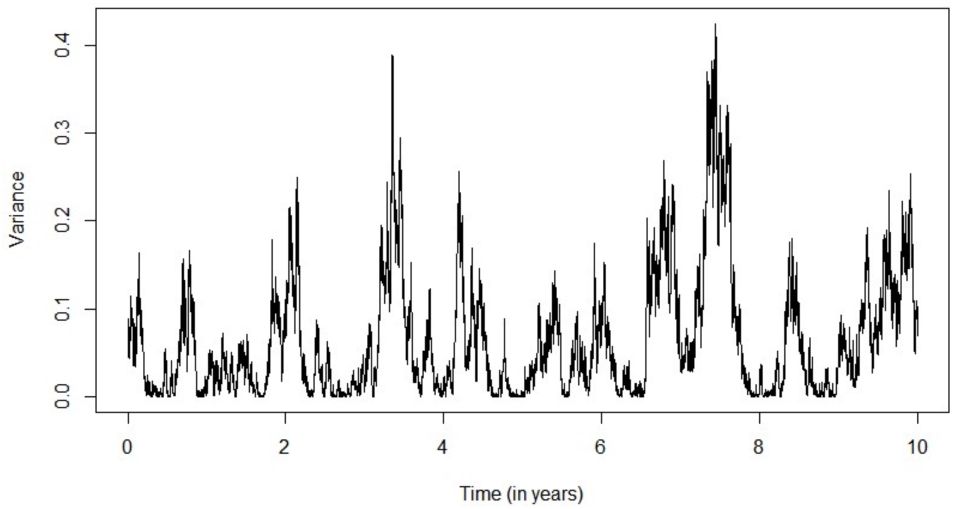

Figure 6.1: One sample path of the variance process under the Heston model

- Bates :

We again use the Euler scheme with a full truncation fix for the variance process as in the Heston model. However, the discretization scheme of the price process is replaced by :

$$S_{t_{i+1}} = S_{t_i}\left(1 + r\Delta t + \sqrt{v_{t_i}}\sqrt{\Delta t}\,\varepsilon_{S,t_i} + (Y_i - 1)\,\Delta N_{t_i}\right) \tag{6.3}$$

where $Y_i \sim \text{Log}N(\mu_j, \sigma_j^2)$ and $\Delta N_{t_i} \sim Poi(\lambda\,\Delta t)$.

- Rough Heston :

The discretized price process is exactly the same as in the Heston model with (6.1). We then simply use an Euler discretization scheme for the variance process (3.13) of the rough Heston. At current time $t = 0$, we hence write for $i = 0, ..., n$ with $t_0 = 0$ and $t_n = T$:

$$v_{t_i} = \xi_0(t_i) + \frac{1}{\Gamma(H+1/2)}\sum_{k=0}^{i}(t_i - t_k)^{H-1/2}\nu\sqrt{v_{t_k}}\,\sqrt{\Delta t}\,\varepsilon_{v,t_k} \tag{6.4}$$

One sample path of the variance process over 10 years under our calibrated rough Heston model is plotted in Fig. 6.2. We clearly see the rough behavior of the variance process compared to the sample paths of the Bates and Heston models. We also have that the vol-of-var parameter ν is quite high, leading to large movements in the variance process.

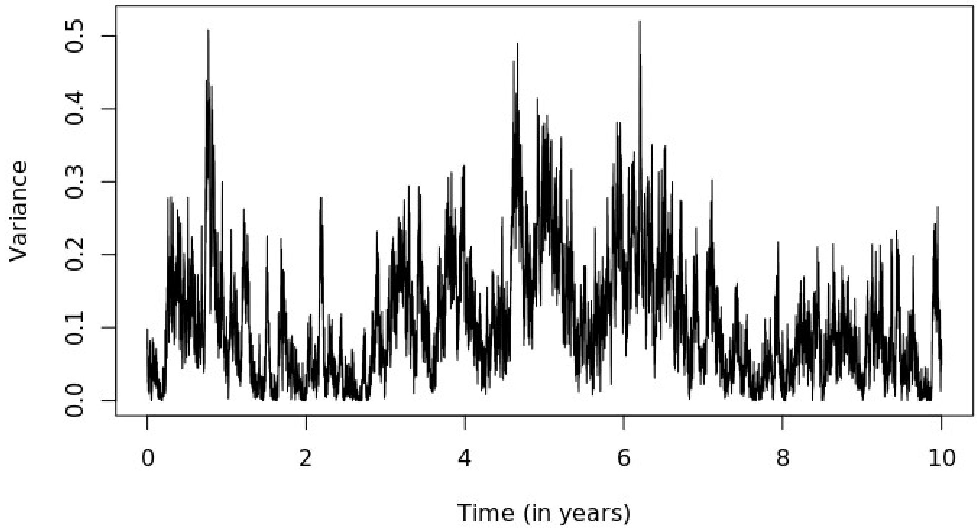

Figure 6.2: One sample path of the variance process under the rough Heston model

- rBergomi :
The price process is again given by (6.1). However, the variance process is now simply given by :

$$v_{t_i} = \xi_0(t_i)\, \mathcal{E}\left(\eta\, \tilde{W}^*_{t_i}\right)$$

where we use the market forward variance curve for $\xi_0(t_i)\,(= \mathbb{E}^{\mathbb{P}^*}[v_{t_i}])$ and the hybrid scheme (4.3) for the simulation of $\tilde{W}^*_{t_i}$, with $i = 0, ..., n$. You can also find in Fig. 6.3, one simulated sample path of the rBergomi variance process using this Hybrid scheme. Due to the huge vol-of-var parameter η, the variance paths tend to explode and exceed 100%. Generated sample paths with the rBergomi are therefore not realistic. Furthermore, if we compute the sample variance $\mathbb{V}_{\mathbb{P}^*}(v_t)$, we would obtain the exact same shape as in Fig. 12.1, which confirms the non-stationary property of the variance process in the rBergomi. The roughness of the variance process is again clearly visible.

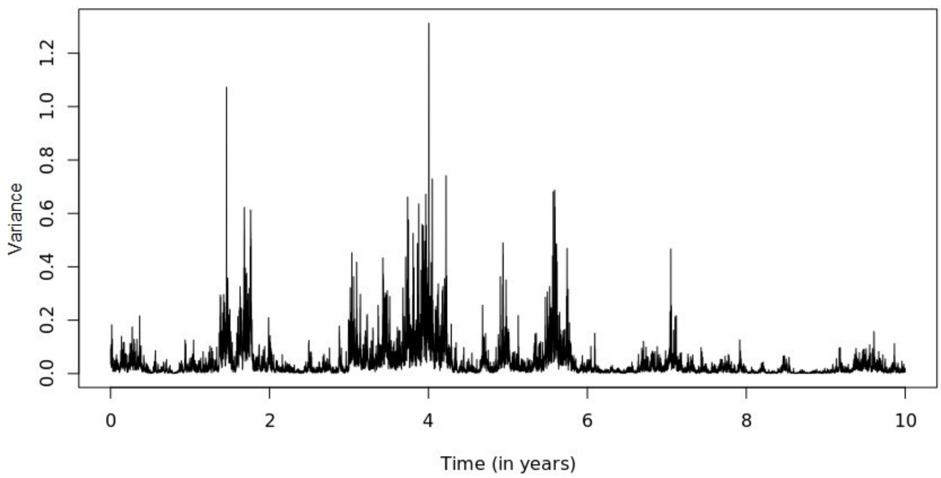

Figure 6.3: One sample path of the variance process under the rBergomi model

Finally, for the rough Heston and the rBergomi, we simply use an absorption fix when dealing with negative variance. With this fix, it can be verified for both models that the mean of our m simulations of the variance process $(v_t)_{t\geq 0}$ gives us back the forward variance curve $\xi_0(t)$.

7. Conclusion of the fit

From the analyses of the implied volatility surface, we can conclude that rough volatility models with the rough Heston and the rBergomi clearly outperform standard SV models in terms of goodness of fit of the observed term structure of the ATM volatility skew. Therefore, with a RMSE of 0.0923 and a good fit of the implied volatility surface, we conclude that the rough Heston is the best of the considered models. Combined with the fact that it exhibits a rough variance process (with a H very close to the historical estimate), this model can hence reproduce numerous statistical properties of the spot volatility process and provide highly accurate and consistent results. Moreover, we can build at large time scales a stationary regime for the volatility in the rough Heston which ensures a reasonable long-term behavior of the model. Finally, the rough Heston is also particularly tractable (only three parameters to calibrate and a characteristic function available in quasi-closed form) which is very important in practice for calibration and option pricing. To quote Gatheral from the 18^{th} Winter school of Mathematical Finance (2019, Lunteren) : *"For perhaps the first time, we have a simple consistent model of historical and implied volatilities"*.

Concerning the rBergomi model, even with calibrated parameters, it provides a higher RMSE than in the other models and hence a less good fit of the observed option prices (at least in our implementation with the market forward variance curve). The rBergomi does not provide realistic sample paths in the long run due to the huge level of the vol-of-var parameter and an exploding quantity $\mathbb{V}^{\mathbb{P}^*}[v_u|\mathcal{F}_t]$ for large u. Furthermore, this model is fairly slow in terms of running time. To quote El Euch et al. [13]: *"Even with the introduction of the efficient hybrid scheme [of Bennedsen et al. [7]], practical implementation [of the rBergomi model] has proved to be difficult."* One solution to improve the efficiency of this pricing model is to use asymptotics such as in Fukasawa [16], in Forde and Zhang [15] or in Bayer et al. [4]. Finally, Bayer et al. [5] propose a neural network approach to calibrate more accurately the rBergomi and to approximate the implied volatility surface. We will however not deepen these methods in this paper.

8. Life insurance contract valuation

Although all models are well calibrated and hence vanilla options have approximately the same prices under all models, exotic option prices can differ dramatically. It is important to point out that vanilla options determine the marginal distribution (at maturity T of the option), not the process. Indeed, the underlying fine-grain properties of the process have an important impact on path-dependent option prices. We now highlight the impact of exotic price ranges between our four calibrated models by valuating our endowment life insurance contract described in section 2. This way, we can compare more thoroughly the rBergomi and the rough Heston models in terms of long-term properties. For further reference on equity-linked endowment valuation, we refer to Bacinello et al. [2].

8.1. Valuation

By the first fundamental theorem of asset pricing, the fair value at time $t = 0$ of the cash-flow F_t^e in (2.1) is given by its discounted expected value under a risk-neutral measure $\mathbb{P}^*$.

However, this cash flow also depends on the path of the Poisson process $(N_t)_{t\geq 0}$ which is not known at time $t = 0$. Therefore, we take the following expectation conditionally to the filtration $\mathcal{G}_0$ to obtain the fair value of our equity-linked endowment contract :

$$FV_0 = \mathbb{E}\left[(1 - N_T)\, e^{-rT}\, \mathbb{E}^{\mathbb{P}^*}[F_T^s \,|\, \mathcal{F}_0] + \int_0^T e^{-rt}\, \mathbb{E}^{\mathbb{P}^*}[F_t^d \,|\, \mathcal{F}_0]\, dN_t \,\middle|\, \mathcal{G}_0\right]$$

The processes $(N_t)_{t\geq 0}$ and $(S_t)_{t\geq 0}$ being independent, we obtain that:

$$FV_0 = \,_Tp_x\, e^{-rT}\, \mathbb{E}^{\mathbb{P}^*}[F_T^s] + \int_0^T e^{-rt}\, \mathbb{E}^{\mathbb{P}^*}[F_t^d]\, _tp_x\, \mu_x(t)\, dt$$

We now want to price this insurance contract with the four models we calibrated above (Heston, Bates, rBergomi and rough Heston). We can then use a Monte-Carlo approach to simulate their price process $(S_t)_{t\geq 0}$ (and variance process) and take the average of the paid benefit under each simulation $j = 1, ...m$ in order to derive the expectation under $\mathbb{P}^*$, *i. e.* :

$$FV_0 = \frac{1}{m}\sum_{j=1}^{m}\left(e^{-rt_n} F_{t_n,j}^s\, \mathbb{1}\left\{\sum_{i=0}^{n} \Delta N_{t_i,j} = 0\right\} + \sum_{i=0}^{n} e^{-rt_i} \Delta N_{t_i,j}\, F_{t_i,j}^d\, \mathbb{1}\left\{\sum_{k=0}^{i-1} \Delta N_{t_k,j} = 0\right\}\right)$$

where the price process $(S_t)_{t\geq 0}$ in F_t^e is defined by the risk-neutral pricing equation of each model. The discretization of their price process and variance process is given in the previous Section 6. Moreover, the use of a Poisson process above makes it easy to add the mortality effect in the simulations to compute FV_0. Indeed, for each simulation $j \in m$, we generate $n = T/\Delta t = 5/0.001 = 5000$ Poisson random variables $\Delta N_{t_i,j}$ with parameter $\lambda = \mu_x(t_i)\,\Delta t$ for $i = 0, ..., n$. For the first i where $\Delta N_{t_i,j} = 1$, we compute a death benefit $F_{t_i,j}^d$ and if $\Delta N_{t_i,j} = 0$ for all i, we compute a survival benefit $F_{t_n,j}^s$.

We consider the following contracts :

- A female policyholder aged $x = 50$ or $x = 65$ at time $t = 0$.
- We use the Belgian regulatory life table FR for the Makeham force of mortality $\mu_x(t)$.
- The initial amount F_0 invested in the fund equals 10 000 €.
- The policyholder pays a unique premium P at time $t = 0$. Note that we could have imposed in the following that $FV_0 = P = F_0 = 10\ 000$ € so as to make the contract *fair* and then determine the corresponding κ_g, κ_m or η in (2.1) that verifies this condition. However, since we aim to compare the contract's value FV_0 between models, we prefer to fix arbitrary values for κ_g, κ_m and η and then derive the corresponding value of the contract.
- We then assume the following parameters in Table 8.1 when valuating the contract:

N° of contract	Gender	Initial age	κ_g	κ_m	η	Maturity T
1)	Female	50	0.01	0.2	0.8	5
2)	Female	50	0.01	0.2	0.8	10
3)	Female	50	0.01	0.2	0.4	10
4)	Female	50	0.01	0.4	0.8	10
5)	Female	65	0.01	0.2	0.8	15

Table 8.1: Parameters of the equity-linked endowments

We obtain in Table 8.2 the fair values of the endowments with our different models using Monte-Carlo simulations with $m = 200\,000$ and working with the market forward variance curve $\xi_0(t)$:

N° of contract	**Heston**	**Bates**	**rBergomi**	**rough Heston**
1)	14 036.57 €	13 457.49 €	12 291.17 €	12 288.43 €
2)	19 372.58 €	17 697.79 €	14 909.54 €	14 055.86 €
3)	14 999.76 €	14 301.43 €	12 834.84 €	12 628.43 €
4)	20 872.07 €	19 108.38 €	15 197.75 €	14 701.38 €
5)	24 925.05 €	21 856.70 €	17 013.96 €	15 425.35 €

Table 8.2: Fair value of the endowment contracts with $\xi_0(t)$

We can compare Table 8.2 with the following Table 8.3 computed using the constant forward variance curve $\xi_0^{cst}(t) = 0.0925$:

N° of contract	**Heston**	**Bates**	**rBergomi**	**rough Heston**
1)	14 036.57 €	13 457.49 €	12 527.35 €	12 730.91 €
2)	19 372.58 €	17 697.79 €	15 499.17 €	15 154.18 €
3)	14 999.76 €	14 301.43 €	13 261.24 €	13 258.13 €
4)	20 872.07 €	19 108.38 €	16 294.61 €	16 430.41 €
5)	24 925.05 €	21 856.70 €	17 925.66 €	17 286.15 €

Table 8.3: Fair value of the endowment contracts with $\xi_0^{cst}(t)$

We first see that the Heston model leads to a higher price than the Bates model. Indeed, even if the long-term variance is higher in the Bates model, the negative average jumps combined with a lower initial variance v_0, a lower speed of mean reversion λ and a lower vol-of-var parameter ν lead to a lower price in the Bates model. Secondly, we have that rough-type models have a lower price than standard SV models. This can be partly explained in Table 8.2 by the long-term variance equal on average in rough models to $\lim_{t\to\infty} \xi_0(t) = 0.0395$, which is lower than the long-term mean in the Heston and Bates model. However, if we analyze the second Table 8.3, we still have lower prices for rough models even if the long-term variances are this time comparable. This remaining difference can thus be explained by the very long reversion time scale in rough models (cfr [18]) and by the rough properties of the variance process. Moreover, we can see that the rBergomi model tends to have a higher fair value than the rough Heston due to its larger vol-of-var parameter ν and the explosion of $\mathbb{V}^{\mathbb{P}^*}[v_u|\mathcal{F}_t]$ when u is large. This is especially true at long time scales and when the participation rate η is high. Finally, comparing the different contracts, we clearly see that the larger the maturity, the higher is the difference between rough-type models and standard SV models. This will be confirmed with Table 8.5 below. Moreover, when the participation rate η decreases, the fair value of the contract is logically lower since the policyholder earn a lower portion of the yearly returns. This lower η also lead to less pronounced differences between rough and standard SV models since their divergent sample paths properties play a lesser role. We observe the same effect when the maximal yearly return κ_m increases, with higher differences in fair value between rough and standard SV models due to their divergent sample paths.

Since we said that the rough Heston model is the most consistent with risk-neutral data, we retain the fourth column of Table 8.2 as being the contracts' prices which are the most market-consistent. We confirm these effects with the two following Tables 8.4 and 8.5, displaying the fair value FV_0 in function of the minimum yearly guaranteed rate k_g and the maturity of the contract T. These two tables are computed using the market forward variance curve but similar tables derived from the constant curve $\xi_0^{cst}(t)$ can be found in Appendix 11 with Tables 11.1 and 11.2. These two tables in Appendix are also consistent with the following analyses.

$T = 10$	Heston	Bates	rBergomi	rough Heston
$k_g = 0.5\%$	18 951.46 €	17 307.24 €	14 518.48 €	13 638.97 €
$k_g = 1\%$	19 372.58 €	17 696.27 €	14 909.54 €	14 063.09 €
$k_g = 2\%$	20 282.23 €	18 534.77 €	15 785.42 €	15 051.42 €
$k_g = 5\%$	23 664.37 €	21 655.51 €	19 301.23 €	18 969.22 €

Table 8.4: Fair value FV_0 for various k_g with maturity $T = 10$

We observe the highest differences between rough and standard SV models when k_g tends to be small. Indeed, in this case, the minimum yearly guarantee is exercised less often and therefore the yearly returns, which are highly influenced by the sample paths, play a more important role. This thus leads to stronger differences in fair value between models with divergent sample path properties.

$k_g = 1\%$	Heston	Bates	rBergomi	rough Heston
$T = 5$	14 036.57 €	13 457.49 €	12 291.17 €	12 288.43 €
$T = 10$	19 372.58 €	17 696.27 €	14 909.54 €	14 063.09 €
$T = 20$	35 631.76 €	29 613.34 €	20 639.81 €	17 823.38 €

Table 8.5: Fair value FV_0 for various maturities T with $k_g = 1\%$

The differences in fair value between models are also the most exacerbated when the maturity of the contract is large. The impact of the sample paths properties of each model is indeed stronger at longer time scales and the differences in behavior of the long-term variance are exacerbated when the maturity is large, as explained in the previous sections and in 12.2. We finally want to highlight that the numbers given in the tables above can slightly change for each run of simulations but are quite stable with our chosen m, equal to 200 000.

9. Conclusion

Rough fractional stochastic volatility models are excellent candidates for reproducing important stylized facts of the volatility time series and for providing a consistent implied volatility surface with the observed one. In this paper, we explore more closely two tractable implementations of the RFSV model, the rBergomi and the rough Heston and analyze their implications for the pricing of long-term life insurance claims. The properties of these two rough-type models are then compared with standard SV models (Heston and Bates model).

Among these four models, we conclude that the rough Heston is the most consistent with historical and risk-neutral data while enjoying reasonable long-term properties. Indeed, this rough Heston model with $H \approx 0.1$ tends to outperform standard SV models in terms of European option calibration and in terms of fit of the volatility surface. We also retain the rough Heston model as a highly tractable implementation of rough-type models with only three parameters to estimate and a characteristic function available in quasi-closed form, which is not the case of the rBergomi. Combined with the Carr-Madan formula, the calibration and pricing of European options with the rough Heston model is hence extremely fast and accurate. Moreover, we manage to build at large time scales a stationary regime for the volatility process in the rough Heston. This way, we obtain a model with a reasonable behavior for its volatility process in the long run, which overcomes the non-stationary issue of the rBergomi. Using the pricing methodology introduced in this paper, a more accurate fair value of long-term equity-linked life insurance contracts is then obtained in comparison with standard SV models and the rBergomi model, especially for contracts with a large maturity and a low minimum guaranty κ_g. More precisely, we obtain with the rough Heston model a fair value significantly lower than in standard SV models due to the long-reversion time scale and the rough property of volatility.

As future work, we should re-calibrate all the models considered in this paper on other market data of European options. Choosing an other index/stock with a larger set of available maturities and at another point in time should help us to confirm and validate the results derived with our methodology. Through a comparison of the results obtained with the market forward variance curve to the ones obtained with the constant forward variance curve, we see that the choice of this variance curve is of utmost importance. Hence, having a larger set of maturities should especially provide us with a more reliable market forward variance curve and hence a more accurate fair value. Moreover, more advanced mortality models could be considered such as in [21] or in [9].

Appendix

10. Theoretical reminder

10.1. Carr-Madan formula

We here briefly introduce the Carr-Madan formula. Let $k = \log(K)$ the log-strike and $C(k,T)$, the price of a European call of log-strike k and maturity T. Using Fourier transform on $c(k,T) = \exp(\alpha k)C(k,T)$ and then its inverse Fourier transform, Carr and Madan [10] showed that :

$$C(k,T) = \exp(-\alpha k)\frac{1}{\pi}\int_0^\infty \exp(-iuk)\,\psi(u;T)\,du \tag{10.1}$$

where :

$$\psi(u;T) = \frac{\exp(-rT)\Phi(u-(\alpha+1)i,T)}{\alpha^2+\alpha-u^2+i(2\alpha+1)u}$$

with $\Phi(.,T)$ the characteristic function of the log-asset price at maturity T. The integral is typically calculated using a Fast Fourier Transform. Using the FFT, one can actually calculate the prices for a whole range of strikes in one run. The price in between the computed strikes are obtained via interpolation. For more details, we refer to Schoutens [28].

In order to derive model-based implied volatilities from the Carr-Madan Formula for different SV models, we just have to compute $\psi(u;T)$ with the B&S characteristic function, which gives :

$$\psi_{BS}(u;T) = \frac{\exp\left(-rT+iu(\log S_0+rT)\right)\exp\left(-\frac{1}{2}(u-(\alpha+1)i)(u-\alpha\, i)\,\sigma_{BS}^2 T\right)}{\alpha^2+\alpha-u^2+i(2\alpha+1)u}$$

where σ_{BS} is the B&S relative volatility. From the definition of model-based implied volatilities, we must have $C_{BS}(k,T) = C(k,T)$ where $C(k,T)$ is the price of a call option obtained via a specified SV model. It implies that :

$$\int_0^\infty \exp(-iuk)(\psi(u;T) - \psi_{BS}(u;T))\, du = 0$$

Solving this equation with respect to σ_{BS} using FFT allows to derive numerically (and efficiently) the volatility surface for different SV models (using their respective characteristic function). Having a closed (or quasi-closed) form characteristic function of the log-price is therefore a nice property to have for a pricing model.

10.2. Heston model

The Heston model under a risk neutral measure $\mathbb{P}^*$ is given by :

$$dS_t = S_t\, r\, dt + S_t \sqrt{v_t}\, dW_t^* \tag{10.2}$$

$$dv_t = \lambda(\eta - v_t)\, dt + \nu \sqrt{v_t}\, d\hat{W}_t^* \tag{10.3}$$

with W_t^* and $\hat{W}_t^*$ two correlated Brownian motions defined on $(\Omega, \mathbb{P}^*, \mathcal{F})$ such that $\langle W^*, \hat{W}^* \rangle_t = \rho\, t$ with $-1 \le \rho \le 1$, the correlation between the stock and the variance processes. We also have that $S_0 \ge 0$ is the initial stock price, $v_0 = \sigma_0^2 \ge 0$ the initial variance, η is the long-run variance of v_t, λ denotes the speed of mean-reversion and ν the volatility of variance parameter. The instantaneous variance v_t in the Heston model is a CIR process. The Heston characteristic function of the log-stock price $\log(S_t)$ at time t and point u is known in closed-form and given by :

$$\begin{aligned}\Phi(u,t) &= \mathbb{E}\left[\exp\left(iu \log(S_t)\right) | S_0, v_0\right] \\ &= \exp\left(iu(\log S_0 + r\,t)\right) \times \exp\left(\eta\,\kappa\,\theta^{-2}\left((\kappa - \rho\,\theta u i - d)\,t - 2\log\left(\left(1 - g e^{-dt}\right)/(1-g)\right)\right)\right) \\ &\quad \times \exp\left(v_0\,\theta^{-2}\,(\kappa - \rho\,\theta\, iu - d)(1 - e^{-dt})/(1 - g e^{-dt})\right) \end{aligned} \tag{10.4}$$

where :

$$\begin{aligned} d &= \left((\rho\,\theta\, u\, i - \kappa)^2 - \theta^2\left(-iu - u^2\right)\right)^{1/2} \\ g &= (\kappa - \rho\,\theta\, u\, i - d)\,/\,(\kappa - \rho\,\theta\, u\, i + d) \end{aligned}$$

10.3. Bates model

The Bates model, also called SVJ, is given by the following SDE under a risk-neutral measure $\mathbb{P}^*$:

$$\begin{aligned} \frac{dS_t}{S_t} &= (r - \lambda_j\,\xi)\,dt + \sqrt{v_t}\,dW_t^* + (Y-1)\,dN_t \\ dv_t &= \lambda(\eta - v_t)\,dt + \nu\sqrt{v_t}\,d\hat{W}_t^* \end{aligned}$$

where :

- $N_t \sim Poi(\lambda_j\, t)$, a Poisson process with jump intensity $\lambda_j \in \mathbb{R}^+$
- $\log(Y) \sim N(\mu_j, \sigma_j^2)$
- $\xi = \mathbb{E}[Y-1] = e^{\mu_j + \frac{1}{2}\sigma_j^2} - 1$
- $\langle W^*, \hat{W}^* \rangle_t = \rho\, t$ and W_t^*, $\hat{W}_t^*$ are independent from N_t and from Y
- N_t and Y are independent

As for the Heston model, the characteristic function of the log-stock price is known in closed-form :

$$\begin{aligned}\Phi(u,t) = &\exp\left(iu(\log S_0 + r\,t) - \frac{1}{2}u(u+i)\sigma^2 t\right) \\ &\times \exp\left\{-\lambda\, t\left[iu\left(e^{\mu_j + \frac{1}{2}\sigma_j^2} - 1\right) - \left(e^{iu\mu_j - u^2\sigma_j^2/2} - 1\right)\right]\right\}\end{aligned}$$

11. Constant forward variance curve

11.1. Rough Heston

Using the constant forward variance curve $\xi_0^{cst}(t) = 0.0925$, we find a RMSE of 0.11097 with the initial set of parameters (0.1, 0.2, -0.8). This leads to the following values Θ^*:

H^*	ν^*	ρ^*
0.1235	0.6384	-0.6415

The fit is thus poorer than with the initial forward variance curve derived from the market. The vol-of-var paramater ν^* is now higher and the anti-correlation ρ^* less strong. We again obtain a Hurst index close to the historical estimate.

11.2. rBergomi

Using $\xi_0^{cst}(t) = 0.0925$, we find a RMSE of 0.0851 with the initial set of parameters (0.1, 1.5, -0.9). This leads to the following values Θ^*:

H^*	η^*	ρ^*
0.1231	1.8636	-0.8951

Hence, we obtain the best fit among all the tested models (even better than the Bates model with its 8 parameters). This is due to the fact that the constant $\xi_0^{cst}(t) = 0.0925$ is close to the optimal value (= 0.0915) of the constant forward variance curve that we would obtain if we aimed to minimize the RMSE of the rBergomi with an additional model parameter controlling the level of this curve. However, we have an even higher vol-of-var parameter :

$$\nu^* = \eta^* \sqrt{2H^*}/(2\, C_H) = 1.137$$

This huge level ν^* again leads to unrealistic sample paths. Moreover, we still have a stability issue when calibrating this rBergomi model with a high variability of the results in function of the chosen number of paths and steps (here, $m = 1\,000\,000$ and $n = 300$ for the calibration).

For both models, we again obtain a good fit of the term structure of ATM volatility skew as pictured in Fig. 11.1. Moreover, the two Tables 11.1 and 11.2, display the fair value FV_0 in function of the minimum yearly guaranteed rate k_g and the maturity of the contract T.

$T = 10$	Heston	Bates	rBergomi	rough Heston
$k_g = 0.5\%$	18 951.46 €	17 307.24 €	15 086.55 €	14 753.37 €
$k_g = 1\%$	19 372.58 €	17 696.27 €	15 492.96 €	15 145.61 €
$k_g = 2\%$	20 282.23 €	18 534.77 €	16 403.19 €	16 063.00 €
$k_g = 5\%$	23 664.37 €	21 655.51 €	20 015.25 €	19 818.95 €

Table 11.1: FV_0 for various k_g with maturity $T = 10$ and $\xi_0^{cst}(t)$

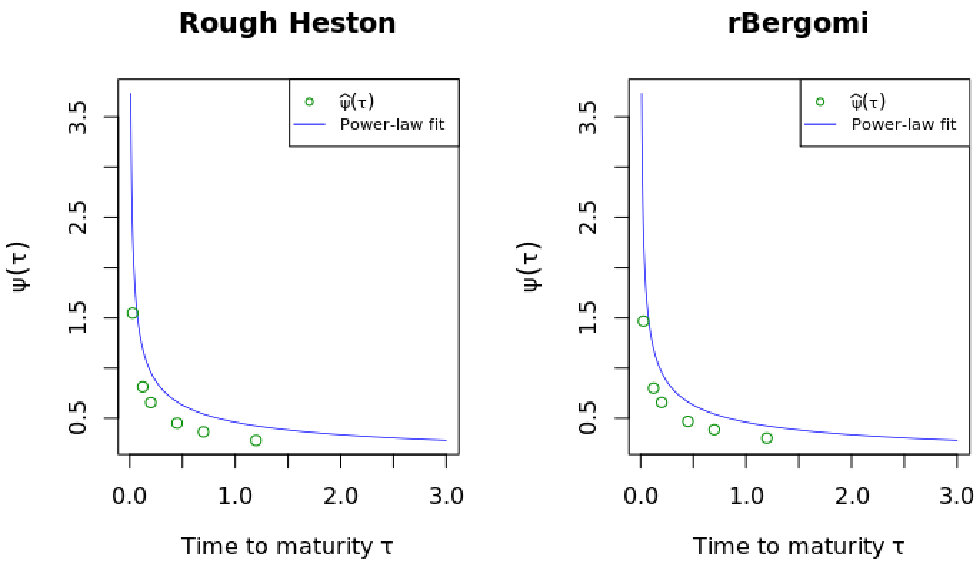

Figure 11.1: Empirical fit (blue) vs. rough Heston and rBergomi fit (green) of $\psi(\tau)$, CAC 40

$k_g = 1\%$	Heston	Bates	rBergomi	rough Heston
$T = 5$	14 036.57 €	13 457.49 €	12 527.35 €	12 730.91 €
$T = 10$	19 372.58 €	17 696.27 €	15 492.96 €	15 145.61 €
$T = 20$	35 631.76 €	29 613.34 €	22 079.51 €	20 350.1 €

Table 11.2: FV_0 for various maturities T with $k_g = 1\%$ and $\xi_0^{cst}(t)$

12. Figures

12.1. Risk-free rates

Maturity	**Rate**	**Maturity**	**Rate**
Overnight	-0.55486 %	8 years	-0.26535 %
7 days	-0.52686 %	9 years	-0.23026 %
1 month	-0.494 %	10 years	-0.19118 %
2 months	-0.44157 %	11 years	-0.15312 %
3 months	-0.43514 %	12 years	-0.11707 %
6 months	-0.35386 %	13 years	-0.08303 %
1 year	-0.36767 %	14 years	-0.07203 %
2 years	-0.38775 %	15 years	-0.02600 %
3 years	-0.39076 %	16 years	-0.00200 %
4 years	-0.37771 %	17 years	0.00099 %
5 years	-0.35563 %	18 years	0.0020 %
6 years	-0.33054 %	19 years	0.01100 %
7 years	-0.29945 %	20 years	0.03599 %

Table 12.1: European risk-free interest rates between 0 and 20 years

12.2. Conditional variance process

For the rBergomi, the variance process is conditionally log-normal and we can prove that:

$$\mathbb{V}_{\mathbb{P}^*}[v_u|\mathcal{F}_t] = \xi_t(u)^2 \left(\exp\left(\eta^2(u-t)^{2H}\right) - 1\right) \tag{12.1}$$

For the rough Heston, if we make the assumption that v_s in equation (3.13) is constant and fixed to $\lim_{u\to\infty} \xi_0(u) = 0.03954$ (which is indeed the case when the time to maturity is above 6 years), we obtain that the variance process is conditionally normal and we can then derive the following expression :

$$\mathbb{V}_{\mathbb{P}^*}[v_u|\mathcal{F}_t] = \frac{0.03954^2\ \nu^2}{[\Gamma(H+1/2)]^2\ 2H}\,(u-t)^{2H} \tag{12.2}$$

Using the market forward variance curve $\xi_0(u)$ in 12.1 with $\eta = 1.416$ and $H = 0.12$ and using $\nu = 0.413$ and $H = 0.12$ in equation 12.2 , we obtain the following figure Fig. 12.1 with $t = 0$.

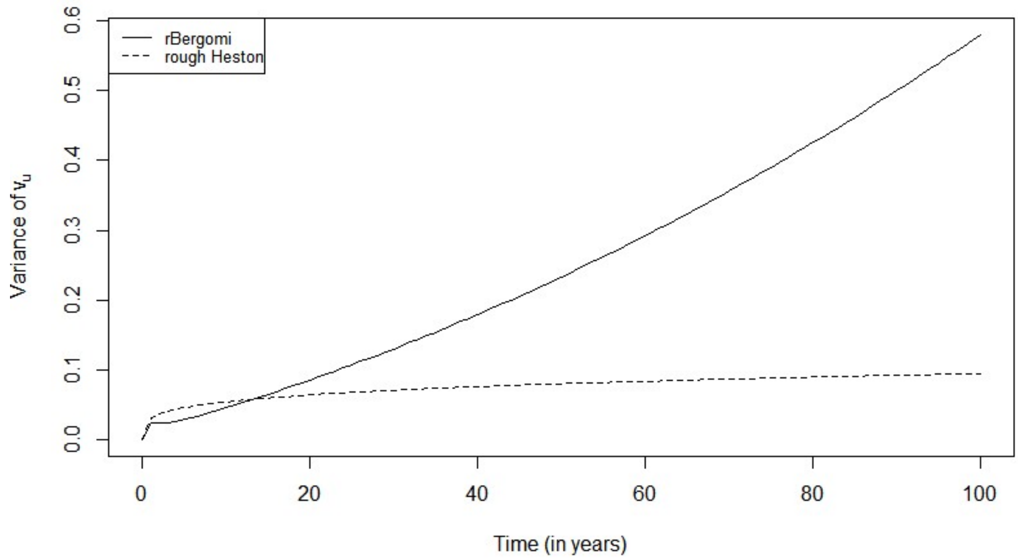

Figure 12.1: Comparison of $\mathbb{V}_{\mathbb{P}^*}[v_u|\mathcal{F}_0]$ in function of u between the rough Heston and the rBergomi models

12.3. ATM volatility skew term structure

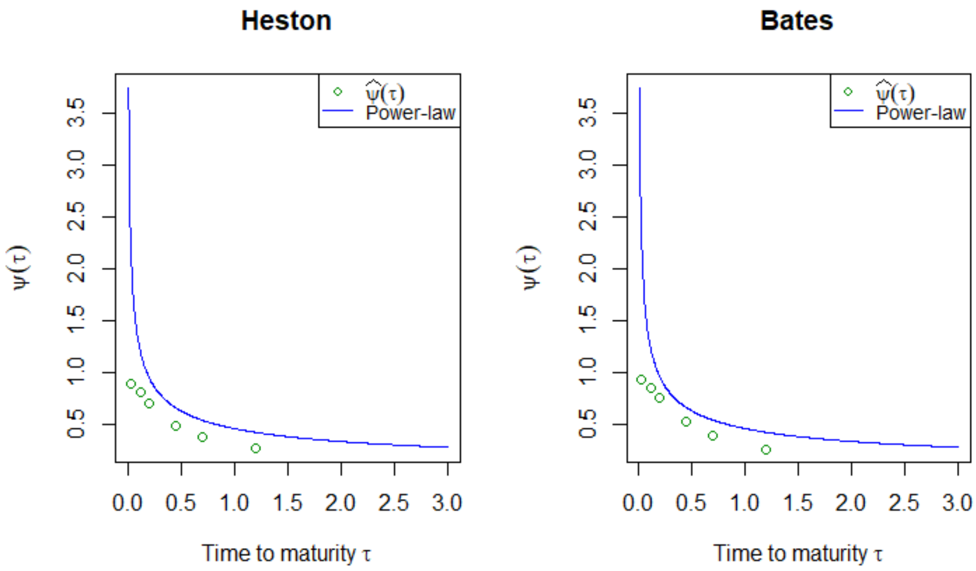

Figure 12.2: Empirical fit (blue) vs. Heston and Bates fit (green) of $\psi(\tau)$, CAC 40

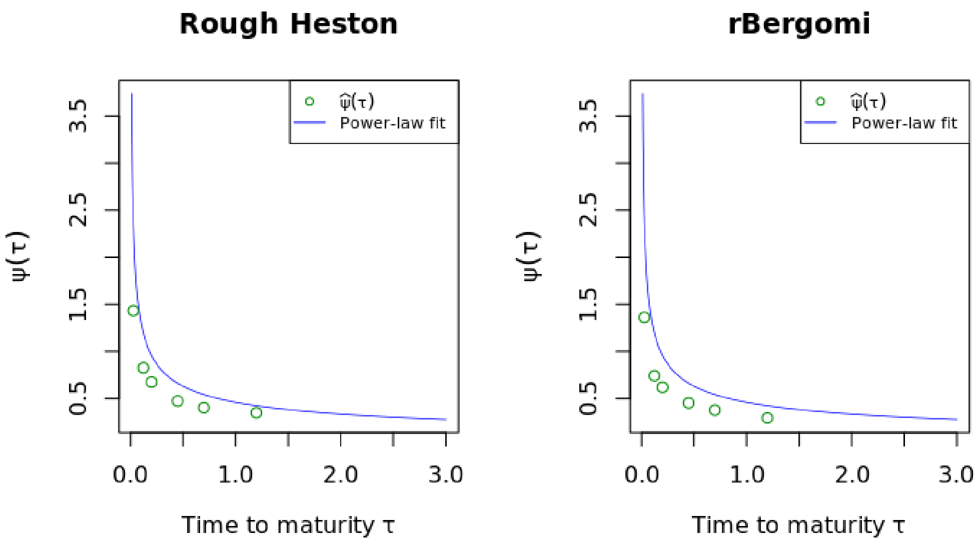

Figure 12.3: Empirical fit (blue) vs. rough Heston and rBergomi fit (green) of $\psi(\tau)$, CAC 40

Availability of data and material The datasets and code generated during and/or analysed during the current study are available from the corresponding author on reasonable request.

Conflict of interest The authors declare that they have no conflict of interest.

References

[1] Andersen, T.G., Bollerslev, T., Diebold, F.X., Ebens, H.: The distribution of realized stock return volatility. Journal of financial economics **61**(1), 43–76 (2001)

[2] Bacinello, A.R., Biffis, E., Millossovich, P.: Regression-based algorithms for life insurance contracts with surrender guarantees. Quantitative Finance **10**(9), 1077–1090 (2010)

[3] Bayer, C., Friz, P., Gatheral, J.: Pricing under rough volatility. Quantitative Finance **16**(6), 887–904 (2016)

[4] Bayer, C., Friz, P.K., Gulisashvili, A., Horvath, B., Stemper, B.: Short-time near-the-money skew in rough fractional volatility models. Quantitative Finance **19**(5), 779–798 (2019, a)

[5] Bayer, C., Horvath, B., Muguruza, A., Stemper, B., Tomas, M.: On deep calibration of (rough) stochastic volatility models. arXiv preprint arXiv:1908.08806 (2019, b)

[6] Bennedsen, M., Lunde, A., Pakkanen, M.S.: Decoupling the short-and long-term behavior of stochastic volatility. arXiv preprint arXiv:1610.00332 (2016)

[7] Bennedsen, M., Lunde, A., Pakkanen, M.S.: Hybrid scheme for brownian semistationary processes. Finance and Stochastics **21**(4), 931–965 (2017)

[8] Bergomi, L., Guyon, J.: Stochastic volatility's orderly smiles. Risk **25**(5), 60 (2012)

[9] Cairns, A.J., Blake, D., Dowd, K.: Modelling and management of mortality risk: a review. Scandinavian Actuarial Journal **2008**(2-3), 79–113 (2008)

[10] Carr, P., Madan, D.: Option valuation using the fast fourier transform. Journal of computational finance **2**(4), 61–73 (1999)

[11] Cheridito, P., Kawaguchi, H., Maejima, M.: Fractional ornstein-uhlenbeck processes. Electronic Journal of probability **8** (2003)

[12] Comte, F., Renault, E.: Long memory in continuous-time stochastic volatility models. Mathematical finance **8**(4), 291–323 (1998)

[13] El Euch, O., Gatheral, J., Rosenbaum, M.: Roughening heston. Risk pp. 84–89 (2019)

[14] El Euch, O., Rosenbaum, M.: The characteristic function of rough heston models. Mathematical Finance **29**(1), 3–38 (2019)

[15] Forde, M., Zhang, H.: Asymptotics for rough stochastic volatility models. SIAM Journal on Financial Mathematics **8**(1), 114–145 (2017)

[16] Fukasawa, M.: Short-time at-the-money skew and rough fractional volatility. Quantitative Finance **17**(2), 189–198 (2017)

[17] Gatheral, J.: The volatility surface: a practitioner's guide, vol. 357. John Wiley & Sons (2011)

[18] Gatheral, J., Jaisson, T., Rosenbaum, M.: Volatility is rough. Quantitative Finance **18**(6), 933–949 (2014)

[19] Gatheral, J., Keller-Ressel, M.: Affine forward variance models. Finance and Stochastics **23**(3), 501–533 (2019)

[20] Gatheral, J., Radoičić, R.: Rational approximation of the rough heston solution. International Journal of Theoretical and Applied Finance **22**(03), 1950010 (2019)

[21] Hainaut, D., Devolder, P.: Mortality modelling with lévy processes. Insurance: Mathematics and Economics **42**(1), 409–418 (2008)

[22] Karatzas, I., Shreve, S.E.: Brownian motion. In: Brownian Motion and Stochastic Calculus, pp. 47–127. Springer (1998)

[23] Lord, R., Koekkoek, R., Dijk, D.V.: A comparison of biased simulation schemes for stochastic volatility models. Quantitative Finance **10**(2), 177–194 (2010)

[24] Mandelbrot, B.B., Van Ness, J.W.: Fractional brownian motions, fractional noises and applications. SIAM review **10**(4), 422–437 (1968)

[25] McCrickerd, R., Pakkanen, M.S.: Turbocharging monte carlo pricing for the rough bergomi model. Quantitative Finance **18**(11), 1877–1886 (2018)

[26] Moyaert, T., Petitjean, M.: The performance of popular stochastic volatility option pricing models during the subprime crisis. Applied Financial Economics **21**(14), 1059–1068 (2011)

[27] Ninomiya, S., Victoir, N.: Weak approximation of stochastic differential equations and application to derivative pricing. Applied Mathematical Finance **15**(2), 107–121 (2008)

[28] Schoutens, W.: The world of vg. In: Actuarial and financial mathematics conference, pp. 32–38 (2009)